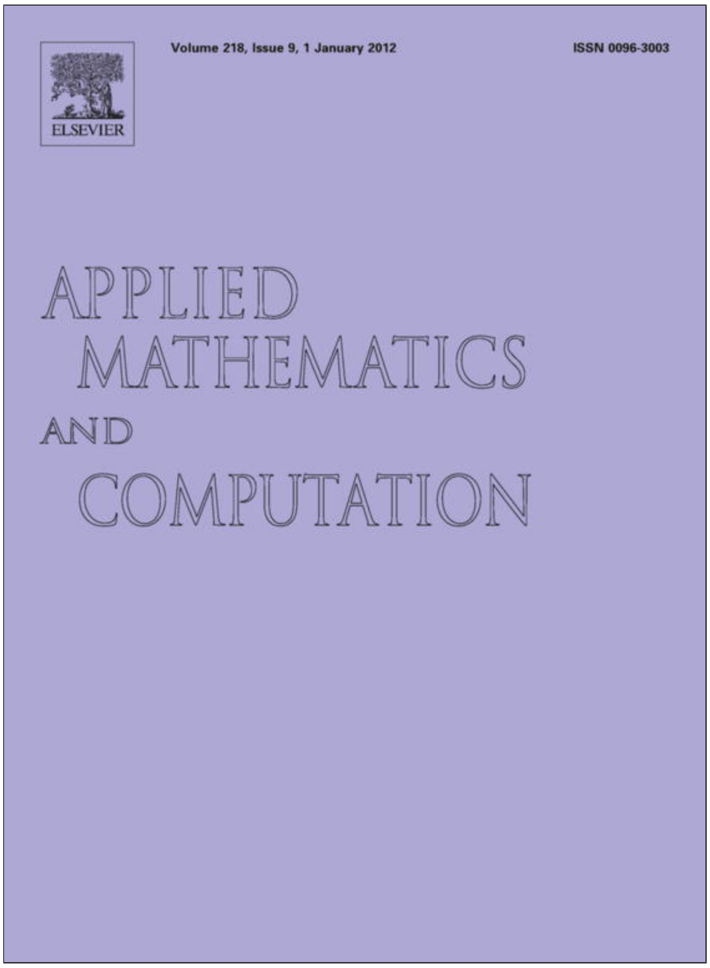
Volume 218, Issue 9, 1 January 2012
ISSN 0096-3003
ELSEVIER
APPLIED MATHEMATICS AND COMPUTATION

Applied Mathematics and Computation 218 (2012) 4684–4694

Contents lists available at SciVerse ScienceDirect

Applied Mathematics and Computation

journal homepage: www.elsevier.com/locate/amc

Numerical continuation methods for studying periodic travelling wave (wavetrain) solutions of partial differential equations

Jonathan A. Sherratt

Department of Mathematics and Maxwell Institute for Mathematical Sciences, Heriot-Watt University, Edinburgh EH14 4AS, UK

ARTICLE INFO

Keywords:
Numerical continuation
Periodic travelling wave
Wave train
Auto
Partial differential equations

ABSTRACT

Periodic travelling waves (wavetrains) are an important solution type for many partial differential equations. In this paper I review the use of numerical continuation for studying these solutions. I discuss the calculation of the form and stability of a given periodic travelling wave, and the calculation of boundaries in a two-dimensional parameter plane for wave existence and stability. I also describe the automated implementation of these numerical continuation procedures via the software package WAVETRAIN (http://www.ma.hw.ac.uk/wavetrain). I conclude by discussing ongoing work on numerical continuation methods for determining the absolute stability of periodic travelling waves.

1. Introduction

Periodic travelling waves (wavetrains) are an important solution type for many partial differential equations (PDEs). They play a fundamental role in the one-dimensional behaviour of self-oscillatory systems [1], for which the complex Ginzburg–Landau equation is the prototype example [2], and they arise in a wide range of other equations including excitable systems [3] and reaction–diffusion–advection equations [4]. As well as this fundamental mathematical role, periodic travelling waves (PTWS) occur in many applications. In physics, PTWS play an important role in hydrodynamics [5–7] and solar cycles [8]. In chemistry, travelling bands were observed in the Belousov–Zhabotinskii reaction more than 30 years ago [9] and are part of the wide range of behaviours seen in oscillatory and excitable chemical reactions [10–12]. In ecology, PTWS have been identified in spatiotemporal data sets on a number of cyclic populations [13–15], and occur on a landscape scale in semi-arid environments, where bands of vegetation moving slowly uphill on gentle slopes are a characteristic feature [16,17].

Like all travelling wave solutions, PTWS are functions of the single variable $z = x - ct$; here t and x are the time and (one-dimensional) space coordinates, and c is the wave speed. This solution ansatz reduces the PDES to an ordinary differential equation (ODE) system, and a PTW is a limit cycle solution of these ODES. However the limit cycle is typically unstable as an ODE solution in both the positive and negative z directions, meaning that it cannot be calculated by direct numerical integration of the ODES. The standard method for calculating a PTW solution is therefore numerical continuation: starting from a Hopf bifurcation in the travelling wave equations, one follows the limit cycle branch until the required PTW solution is reached. Extensions of this approach enable calculation of the regions of parameter space in which PTWS exist. Stability of a PTW can also be determined via numerical continuation, using the method of Rademacher et al. [18] for computing the essential spectrum. In this paper, I will review these different applications of numerical continuation to the study of PTWS, illustrating my remarks via the calculation of boundaries in parameter space for the existence and stability of PTWS in the Klausmeier model for banded vegetation in semi-arid environments [19].

E-mail address: jas@ma.hw.ac.uk

0096-3003/$ - see front matter © 2011 Elsevier Inc. All rights reserved.
doi:10.1016/j.amc.2011.11.005

Some of the methods that I will describe are relatively difficult to implement, even when using an established numerical continuation program such as AUTO [20–23], and this has been a significant barrier to their wider use. In Section 4, I will describe a new software package called WAVETRAIN which uses AUTO to study PTW solutions in an easy-to-use automated way.

2. The Klausmeier model for banded vegetation

In semi-arid environments, vegetation is often self-organised into spatial patterns. A particularly striking manifestation of this is vegetation banding on gentle slopes, in which stripes of grass, shrubs or trees run parallel to the contours, alternating with regions of bare ground [16,17]. A number of mathematical models have been developed for banded vegetation, reflecting the various ecological mechanisms that have been proposed. I will illustrate my discussion of the study of PTWs via the Klausmeier model [19], which has the dimensionless form

$$\partial p/\partial t = \overbrace{\omega p^2}^{\substack{\text{plant}\\ \text{growth}}} - \overbrace{Bp}^{\substack{\text{plant}\\ \text{loss}}} + \overbrace{\partial^2 p/\partial x^2}^{\substack{\text{plant}\\ \text{dispersal}}}, \tag{1a}$$

$$\partial \omega/\partial t = \underbrace{A}_{\text{rain-fall}} - \underbrace{\omega}_{\text{evaporation}} - \underbrace{\omega p^2}_{\substack{\text{uptake}\\ \text{by plants}}} + \underbrace{v\partial \omega/\partial x}_{\substack{\text{flow}\\ \text{downhill}}}. \tag{1b}$$

This was the first PDE model to be proposed for banded vegetation; p and ω are the densities of plant biomass and water, respectively. The parameters A, B and v are dimensionless combinations of a number of ecological parameters, but can be most conveniently interpreted as reflecting mean annual rainfall, plant loss including herbivory, and slope gradient, respectively. A key component of (1) is the nonlinear term ωp^2, which reflects the fact that higher levels of organic matter in the soil, and the presence of roots, increase the infiltration of rain water into the soil [24,25]. A detailed ecological appraisal of the Klausmeier model is given in [26], and mathematical properties of the equations are discussed in [27–30]. Before proceeding, it is important to emphasise that (1) is only one of a number of different mathematical models for banded vegetation; Refs. [31–35] contain a selection of other models, and [36] reviews the modelling literature in this area.

Banded vegetation corresponds to spatial patterns of (1) that move in the positive x direction (uphill) at a constant speed, that is, PTWs. Therefore it is important to understand the constraints on the parameters (A, B, v and wave speed) for PTW solutions of (1) to exist, and for them to be stable.

3. Application of numerical continuation to periodic travelling waves

In this section, I will describe the basic uses of numerical continuation to study the form and existence (Section 3.1) and stability (Section 3.2) of PTW solutions of the partial differential equations

$$\partial \underline{u}/\partial t = \underline{F}(\underline{u}, \partial \underline{u}/\partial x, \partial^2 \underline{u}/\partial x^2, \ldots). \tag{2}$$

I will illustrate my remarks via the Klausmeier model (1); the results I will present on existence of PTWs for (1) have been shown previously in [4], but those on wave stability are new. Throughout this section I will consider only typical, simple behaviour, for which the Klausmeier model provides a good example for the parameter values considered. Moreover, to avoid interfering with readability I will for the most part omit caveats about the possibility of more complicated cases. Rather, in Section 5, I will describe various complications that can arise, and how they can be overcome.

3.1. Periodic travelling wave form and existence

Travelling wave solutions of (2) satisfy

$$c\, d\underline{U}/dz + \underline{F}\left(\underline{U}, d\underline{U}/dz, d^2\underline{U}/dz^2, \ldots\right) = 0 \tag{3}$$

where $\underline{u}(x,t) = \underline{U}(z)$ with $z = x - ct$; c is the wave speed. As discussed in Section 1, a PTW is a limit cycle solution of (3). In simple cases, the limit cycle branch containing this solution is monotonic in the parameters, and has at least one end terminating at a Hopf bifurcation point. For example, Fig. 1 illustrates the branch of PTW solutions of (1) with speed $c = 2$, as a function of the rainfall parameter A. The solution branch emanates from a Hopf bifurcation point at $A \approx 2.78$, and terminates at a homoclinic solution at $A \approx 0.32$. To calculate a PTW solution for a value of A between these limits, one therefore begins by performing a numerical continuation of the steady state, looking for the Hopf bifurcation point. One then switches to the limit cycle solution branch, and numerically continues this branch until the required value of A is reached.

PTW solutions depend on the parameters in the original PDES (2) and also on the wave speed c. If PTW solutions exist for a given set of PDE parameters, then they will do so for a range of values of c [1], with the value of c relevant to a particular PDE solution depending on initial and boundary conditions. Therefore it is natural to consider PTW existence in a parameter plane whose axes are the wave speed c and one of the PDE parameters, referred to henceforth as the "control parameter". For examples of PTW existence visualised in this way, see Refs. [4,39,40].

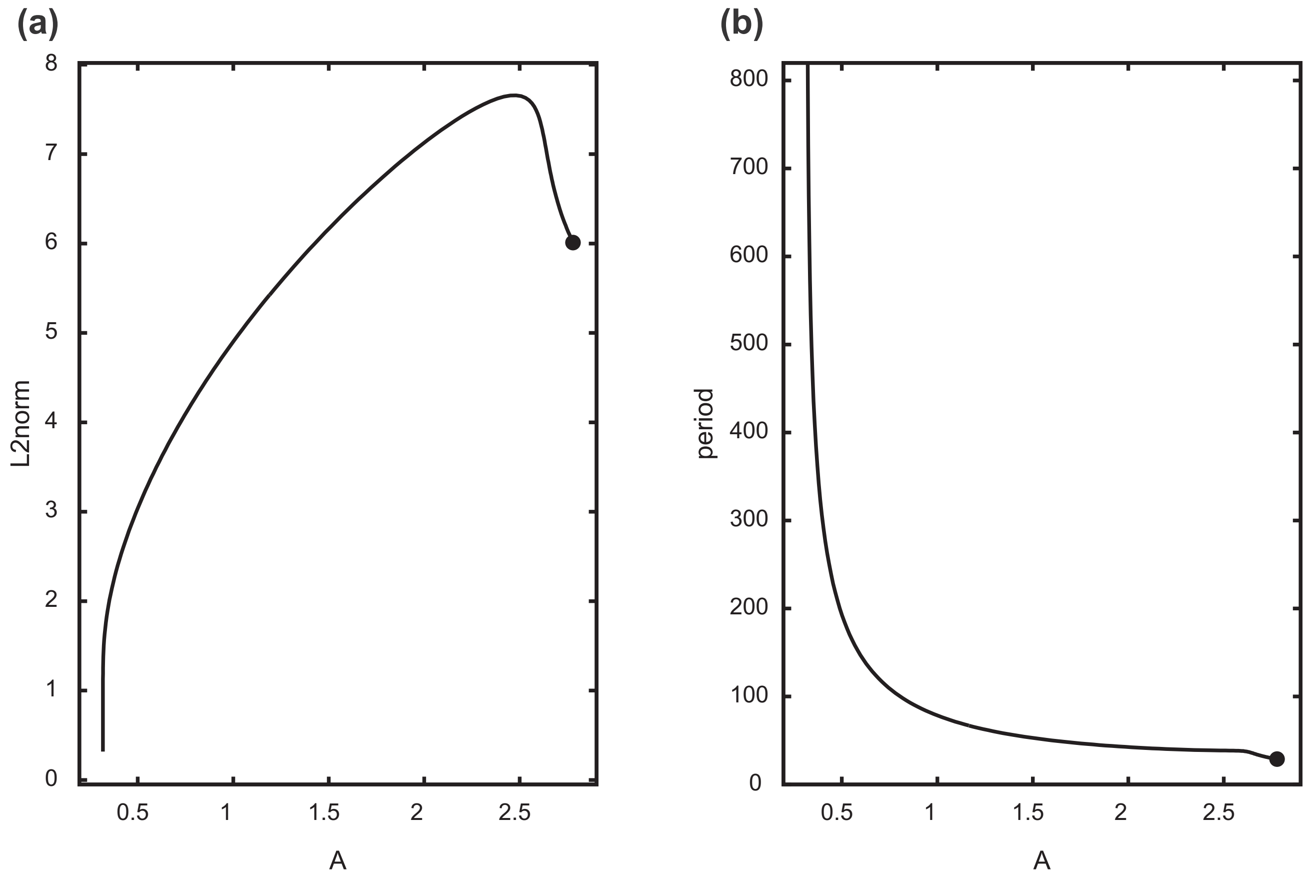

Fig. 1. The branch of PTW solutions of (1) with wave speed $c = 2$, for $B = 0.45$ and $\nu = 182.5$. The branch emanates from a Hopf bifurcation (•) at $A \approx 2.78$, and terminates at a homoclinic solution at $A \approx 0.32$. Part (a) shows the L^2 norm of the solution of the travelling wave ODEs, and (b) shows the period of the wave; both are plotted as a function of the rainfall parameter A. The curves were calculated and plotted using the software package WAVETRAIN [37]. Full details of the WAVETRAIN input files, run commands and plot commands are given at [38].

Typically, the region of the parameter plane in which PTWs exist will be bordered either by a locus of Hopf bifurcation points or a locus of homoclinic solutions. (The other possibility is a locus of folds in the limit cycle solution branch: see Section 5). These loci can be calculated by numerical continuation. For Hopf bifurcation loci this is straightforward. Actual homoclinic loci can be calculated by numerical continuation [41,42], but in practice it is usually easier to approximate the locus by that of a PTW of large period. For example, Fig. 2 illustrates part of the A–c parameter plane for (1); the region in which PTWs exist is bordered on the right by a locus of Hopf bifurcation points, and on the left by a homoclinic locus, which is approximated in the figure by a locus of PTWs with period 2000.

3.2. Periodic travelling wave stability

In applications, it is important to know not only when PTWs exist, but also whether they are stable as solutions of the PDES [15,43]. To study stability, it is convenient to reformulate (2) in terms of z and t. Writing $\underline{\tilde{u}}(z,t) = \underline{u}(x,t)$, (2) becomes

$$\partial\underline{\tilde{u}}/\partial t = c\,\partial\underline{\tilde{u}}/\partial z + \underline{F}\big(\underline{\tilde{u}}, \partial\underline{\tilde{u}}/\partial z, \partial^2\underline{\tilde{u}}/\partial z^2, \ldots\big). \tag{4}$$

For a PTW solution $\underline{\tilde{u}}(z,t) = \underline{U}_{ptw}(z)$ of (4), the equations governing the leading order behaviour of small perturbations are

$$\lambda\,\underline{\widehat{U}} = c\,\partial\underline{\widehat{U}}/\partial z + \underline{\underline{J}} \cdot \underline{\widehat{U}}. \tag{5}$$

Here $\underline{\underline{J}}$ denotes the Jacobian matrix of $\underline{F}$ with respect to $\underline{\tilde{u}}$ and its derivatives, evaluated at $\underline{U}_{ptw}$. Note that the eigenfunction $\underline{\widehat{U}}$ and eigenvalue λ are complex-valued. Eq. (4) are formulated on one period of the PTW, say $0 < z < L$, and the boundary conditions are of key importance. The PTW solution satisfies $\underline{U}_{ptw}(0) = \underline{U}_{ptw}(L)$ by definition, but the eigenfunction need not be periodic: a phase shift is permissible across one period of the wave. Thus the appropriate boundary condition is

$$\underline{\widehat{U}}(L) = \underline{\widehat{U}}(0)\exp(i\gamma) \quad \text{for some} \quad \gamma \in \mathbb{R}. \tag{6}$$

Formally, this boundary condition can be derived using Floquet theory [18,43–45]. Intuitively, the (complex-valued) components of the eigenfunction cannot change in amplitude across one period of the wave, otherwise the eigenfunction would

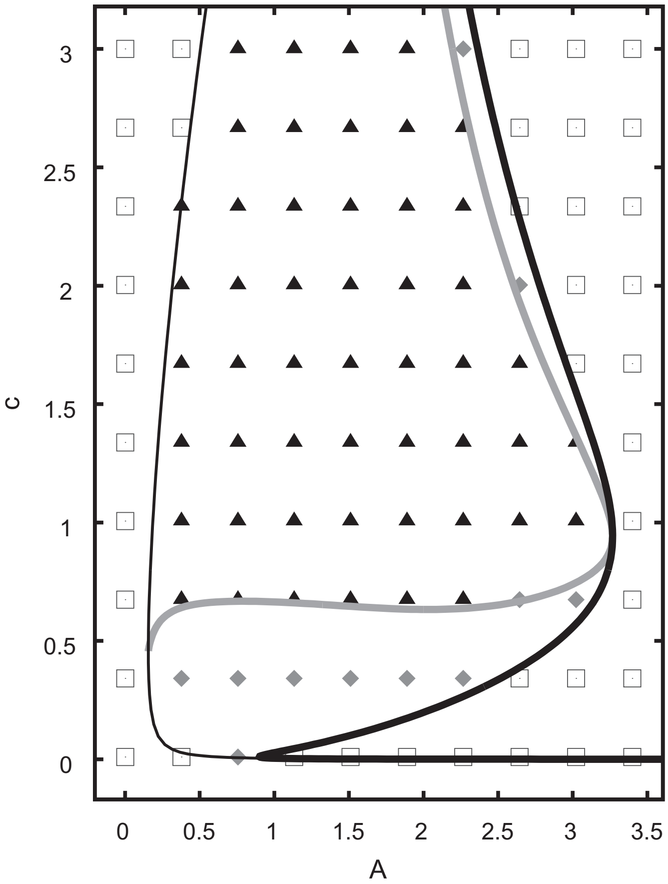

Fig. 2. Existence and stability of PTW solutions of (1) as a function of the rainfall parameter A and the wave speed c, for $B = 0.45$ and $\nu = 182.5$. The symbols show the results from a loop over a 10×10 grid in the parameter plane: ▲ indicates the existence of a stable PTW; ◆ indicates the existence of an unstable PTW; □ indicates that a PTW does not exist. The lines show the boundaries between different regions of the parameter plane. The thick black line is a locus of Hopf bifurcation points in the travelling wave ODEs; the thin black line is a locus of PTWs with period = 2000, which is an approximation to a locus of homoclinic solutions of the travelling wave ODEs; the grey line is the locus of a change in PTW stability, of Eckhaus type. These various points and lines were calculated using the continuation methods described in the main text, implemented via the software package WAVETRAIN [37]. Full details of the WAVETRAIN input files, run commands and plot commands are given at [38].

grow without bound if (5) were considered on $-\infty < z < \infty$. The phase difference must be the same for all components since they are coupled in the linear eigenfunction equations, but otherwise it is unconstrained.

The set of eigenvalues λ for which (5) and (6) has a non-trivial solution is known as the spectrum of the PTW. In general the spectra of linear operators consist of a discrete part (the "point spectrum") and a continuous part (the "essential spectrum"). However for PTWs the point spectrum is always empty [45, Section 3.4.2], and the spectrum consists entirely of the (continuous) essential spectrum. The PTW is unstable if and only if the essential spectrum extends into the right hand half ($\mathrm{Re}\,\lambda > 0$) of the complex plane.

For $\gamma = 0$, (5) can be discretised in z to give a matrix eigenvalue problem, which can be solved by standard numerical methods. Since one is only interested in whether or not there are solutions of (5) and (6) with $\mathrm{Re}\,\lambda > 0$, it is sufficient to calculate a few matrix eigenvalues (10, say) with largest real part, and there are a number of software packages intended for exactly this purpose, for example ARPACK [46,47] which uses a variant of the Arnoldi process. Alternatively, one can simply calculate all of the matrix eigenvalues, for example using routines from LAPACK [48,49], and then select those with the largest real part.

For $\gamma \neq 0$, (5) and (6) cannot be reduced to a matrix eigenvalue problem, but the numerical continuation method of Rademacher et al. [18] can be used. This is a relatively new method, but has proved successful in a variety of different cases (for example [39,50]). One considers the Eqs. (3) and (5) in combination, and performs a numerical continuation in the phase difference γ. The matrix eigenvalues and eigenfunctions calculated for $\gamma = 0$ can be used as starting points for the continuation, which must be done over $0 < \gamma < 2\pi$ for each of the selected matrix eigenvalues (for example the 10 with the largest real part). This traces out the full essential spectrum provided that each of its parts contains a point with $\gamma = 0$. In principle there remains the possibility of islands of spectrum composed entirely of points with $0 < \gamma < 2\pi$. However I am not aware of an example of this, and for many systems including reaction–diffusion equations it can be proved that such islands do not exist [18,45].

Practical implementation of this continuation procedure requires a number of special settings, such as integral constraints to ensure normalisation of the eigenfunction, and full details of these are given in [18]. Fig. 3 shows two spectra calculated in this way for (1); the dots indicate the matrix eigenvalues for $\gamma = 0$. In Fig. 3a the spectrum is confined to the

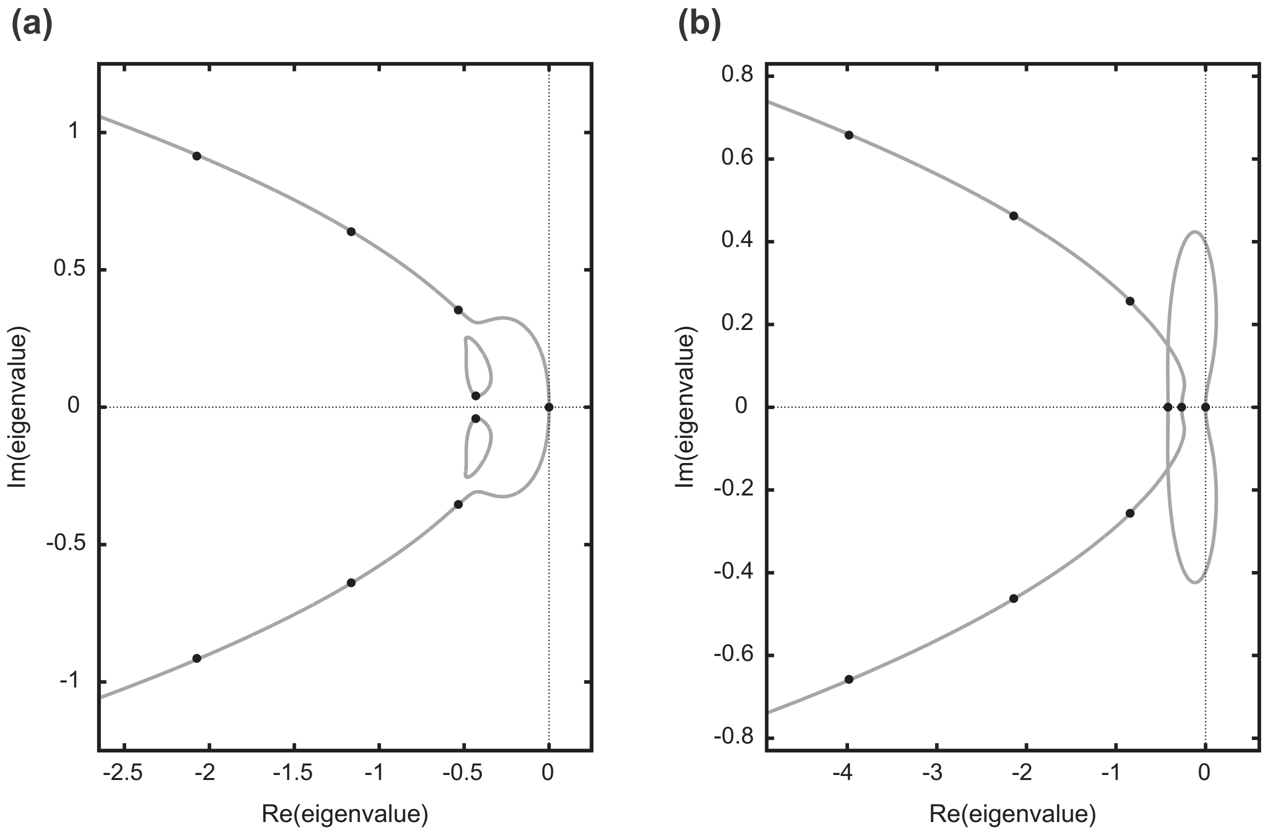

Fig. 3. The essential spectra of two PTW solutions of (1). The grey lines show the spectra and the black dots denote eigenvalues corresponding to eigenfunctions that are periodic with the same period as the PTW. The parameter values are $A = 2.0$, $B = 0.45$, $\nu = 182.5$, with (a) $c = 0.7$ and (b) $c = 0.35$. In (a) the spectrum is confined to the left hand half of the complex plane so that the PTW is stable; in (b) the spectrum crosses the imaginary axis, implying an unstable PTW. The spectra were calculated using the continuation method of Rademacher et al. [18], as described in the main text, implemented via the software package WAVETRAIN [37]. Full details of the WAVETRAIN input files, run commands and plot commands are given at [38].

left-hand half of the complex plane, indicating that the PTW is stable, whereas in Fig. 3b the spectrum crosses the imaginary axis, indicating an unstable PTW.

In both parts of Fig. 3, the origin lies in the spectrum. This is always the case for PTWs, corresponding to their neutral stability to translations. In many cases, including (1), changes from stable to unstable waves as parameters are varied occur via a change in the sign of the curvature of the spectrum at the origin: that is, the stability change is of Eckhaus (sideband) type [53]. A stability change of this type can be located via numerical continuation, and can itself then be numerically continued to give a curve in the control parameter – wave speed plane along which PTW stability changes. This involves numerical continuation of (3) and (5), and the real parts of the first and second derivatives of (5) with respect to γ. Full details of this algorithm are given in [18]; to my knowledge, the only published example of its use is [39], for a system of two reaction–diffusion equations modelling a predator–prey interaction. Fig. 2 shows the boundary between stable and unstable PTW solutions of (1) in the A–c plane, calculated in this way.

To end this section, I mention an alternative method for calculating PTW stability, developed by Deconinck and coworkers [43,51]. This is based on truncating the Fourier–Floquet expansion of the eigenfunction equation ("Hill's Method"), and is particularly well suited to spatially periodic solutions such as PTWs. A "black box" software package implementing the method is available at [52].

4. Implementation in WAVETRAIN

Some of the calculations described in Section 3 are relatively complex. For example, the stability boundary shown in Fig. 2 was calculated using 6 continuation parameters for 15 ODEs subject to 15 boundary conditions and 5 integral constraints. Clearly some previous experience of numerical continuation is necessary before one embarks on a calculation of this type. For the benefit of researchers less familiar with numerical continuation, I have written the software package WAVETRAIN, which performs all of the calculations described in Section 3 in an automated way. Full details of the package, which is freely available and open source (though protected by copyright) are given at [37], and here I provide only a very brief summary.

The input files for WAVETRAIN are text-based, and WAVETRAIN uses them to construct Fortran subroutines that act as input files for the program AUTO [20–23]. Therefore there is no requirement for users to have previous expertise with AUTO or any other programming language or software. WAVETRAIN also includes a plotter, and Figs. 1–5 in this paper were generated by WAVETRAIN.

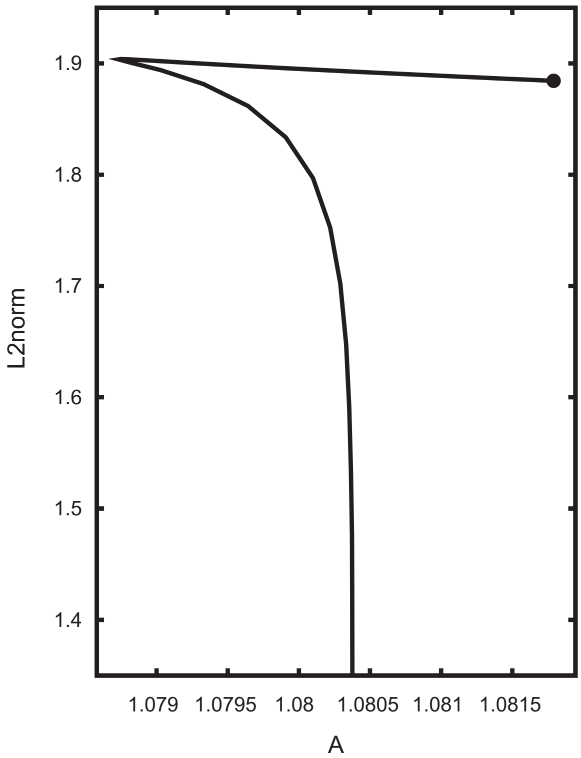

Fig. 4. The branch of PTW solutions of (1) with wave speed $c = 20.3$, for $B = 0.45$ and $\nu = 182.5$. The branch emanates from a Hopf bifurcation (•) at $A = 1.0818$, folds at $A = 1.0787$, and terminates at a homoclinic solution at $A = 1.0804$. The L^2 norm of the solution of the travelling wave ODEs is plotted as a function of the rainfall parameter A. The solution branch was calculated and plotted using the software package WAVETRAIN [37]. Full details of the WAVETRAIN input files, run commands and plot commands are given at [38].

The main WAVETRAIN run commands are as follows:

`bifurcation_diagram`: Performs the computations for a bifurcation diagram, such as that illustrated in Fig. 1. The bifurcation parameter can be either the wave speed or the control parameter. Note that the user specifies which of the PDE parameters is chosen as the control parameter in one of the input files.

`hopf_locus`: Calculates a locus of Hopf bifurcation points. Two pairs of control parameter and wave speed values lying either side of the locus must be supplied as command arguments.

`period_contour`: Calculates a locus of PTWs of constant period. Again, two pairs of control parameter and wave speed values lying either side of the locus must be supplied as command arguments.

`ptw`: Calculates the form of the PTW for given values of the control parameter and wave speed, or returns the information that no PTW exists.

`ptw_loop`: Runs the PTW command over a grid of values in the control parameter – wave speed plane. This is useful to provide starting points for the calculation of Hopf bifurcation loci and contours of constant period.

`stability`: Calculates the form of the PTW for given values of the control parameter and wave speed, and its stability, or returns the information that no PTW exists.

`stability_boundary`: Calculates an interface between stable and unstable PTWs in the control parameter – wave speed plane. Two pairs of control parameter and wave speed values lying either side of the interface must be supplied as command arguments.

`stability_loop`: Runs the `stability` command over a grid of values in the control parameter – wave speed plane. This is useful to provide starting points for the calculation of stability boundaries.

These basic commands are augmented by a variety of others that assist in the preparation of input files and in the management of output data.

5. Potential complications

Although the methods described in Section 3 can be applied directly in many cases, they can be subject to complications. I now summarise these and discuss how they can be overcome.

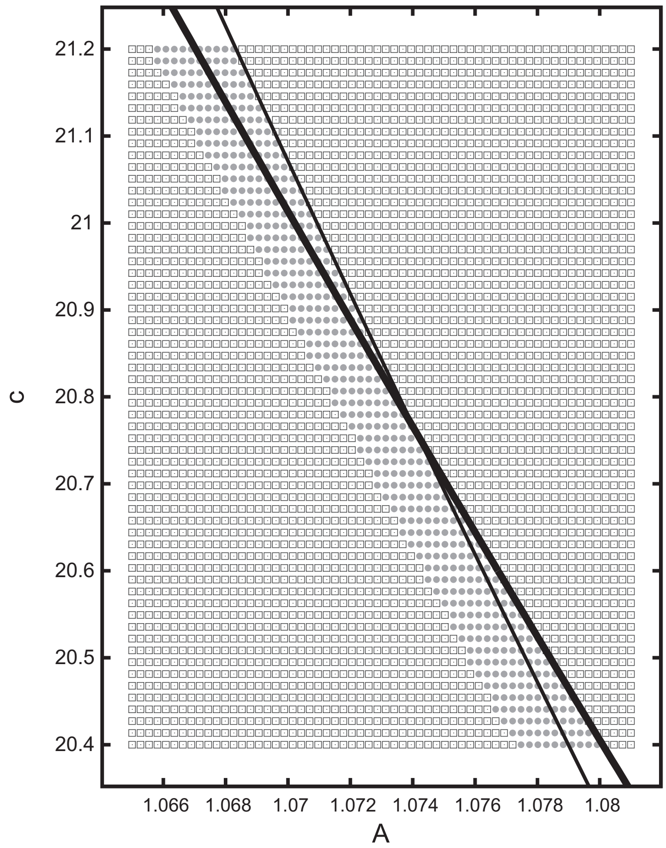

Fig. 5. Existence of PTW solutions of (1) as a function of the rainfall parameter A and the wave speed c, for $B = 0.45$ and $\nu = 182.5$, for a different range of A and c than that used in Fig. 2. Throughout this region of the parameter plane, there is a fold in the PTW solution branch as A is varied for fixed c, as illustrated in Fig. 4. The symbols show the results from a loop over a 60×60 grid in the parameter plane: ● indicates the existence of a PTW; □ indicates that a PTW does not exist. The thick line is a locus of Hopf bifurcation points in the travelling wave ODEs; the thin line is a locus of PTWs with period = 5000, which is an approximation to a locus of homoclinic solutions of the travelling wave ODEs. In contrast to Fig. 2, the parameter region in which PTWs exist is not bordered entirely by the Hopf bifurcation and homoclinic solution loci: rather, the left hand boundary is the locus of the fold in the PTW solution branch (see Fig. 4). The various points and lines were calculated using the continuation methods described in the main text, implemented via the software package WAVETRAIN [37]. Full details of the WAVETRAIN input files, run commands and plot commands are given at [38].

5.1. Equations without time derivatives

One potential complication is that one may wish to study PDEs in which only some equations have time derivatives, with the form

$$\partial u_i/\partial t = F_i(u_i, \partial u_i/\partial x, \partial^2 u_i/\partial x^2, \ldots) \quad 1 \leqslant i < m, \tag{7a}$$
$$0 = F_i(u_i, \partial u_i/\partial x, \partial^2 u_i/\partial x^2, \ldots) \quad m \leqslant i \leqslant N. \tag{7b}$$

This does not present any additional difficulty for any of the continuation computations, but it does affect the calculation of the matrix eigenvalues for $\gamma = 0$, which is the first stage in the determination of PTW stability. Rather than a standard matrix eigenvalue calculation, the problem becomes of generalised type:

$$\lambda \underline{\underline{Y}}\, \underline{u} = \underline{\underline{Z}}\, \underline{u}, \tag{8}$$

where $\underline{\underline{Y}}$ and $\underline{\underline{Z}}$ are $N \times N$ matrices.

In practice the additional difficulty caused by this is only slight, since many standard numerical routines are available for generalised eigenvalue problems. For example, both ARPACK [46,47] and LAPACK [48,49] contain suitable routines. Alternatively one can reduce (8) to a standard eigenvalue problem. In block form (8) can be written as

$$\begin{bmatrix} \underline{\underline{P}} & \underline{\underline{Q}} \\ \underline{\underline{R}} & \underline{\underline{S}} \end{bmatrix} \begin{bmatrix} \underline{v} \\ \underline{w} \end{bmatrix} = \begin{bmatrix} \underline{\underline{I}} & 0 \\ 0 & 0 \end{bmatrix} \begin{bmatrix} \underline{v} \\ \underline{w} \end{bmatrix}, \tag{9}$$

where $\underline{\underline{P}}$ and $\underline{\underline{S}}$ are $(m-1) \times (m-1)$ and $(N-m+1) \times (N-m+1)$ matrices respectively, $\underline{\underline{Q}}$ and $\underline{\underline{R}}$ are rectangular matrices, and $\underline{\underline{I}}$ is the $(m-1) \times (m-1)$ identity matrix; $\underline{v} \in \mathbb{R}^{m-1}$ and $\underline{w} \in \mathbb{R}^{N-m+1}$. Since $\underline{\underline{S}}$ is dominated by its diagonal entries, it will typically be invertible, in which case (9) implies that $\underline{w} = -\underline{\underline{S}}^{-1}\underline{\underline{R}}\underline{v}$. Substituting this back into (8) gives the standard eigenvalue problem

$$\left(\underline{\underline{P}} - \underline{\underline{Q}}\,\underline{\underline{S}}^{-1}\underline{\underline{R}}\right)\underline{v} = \lambda\,\underline{v}.$$

5.2. Folds in the periodic travelling wave solution branch

For the purposes of the discussion in Section 3, I assumed that the PTW solution branch was monotone in the control parameter, so that there is at most one PTW for each pair of control parameter and wave speed values. However, in some cases the solution branch may fold. An example of this is provided by (1) for larger values of c than those considered in Section 3, as illustrated in Fig. 4.

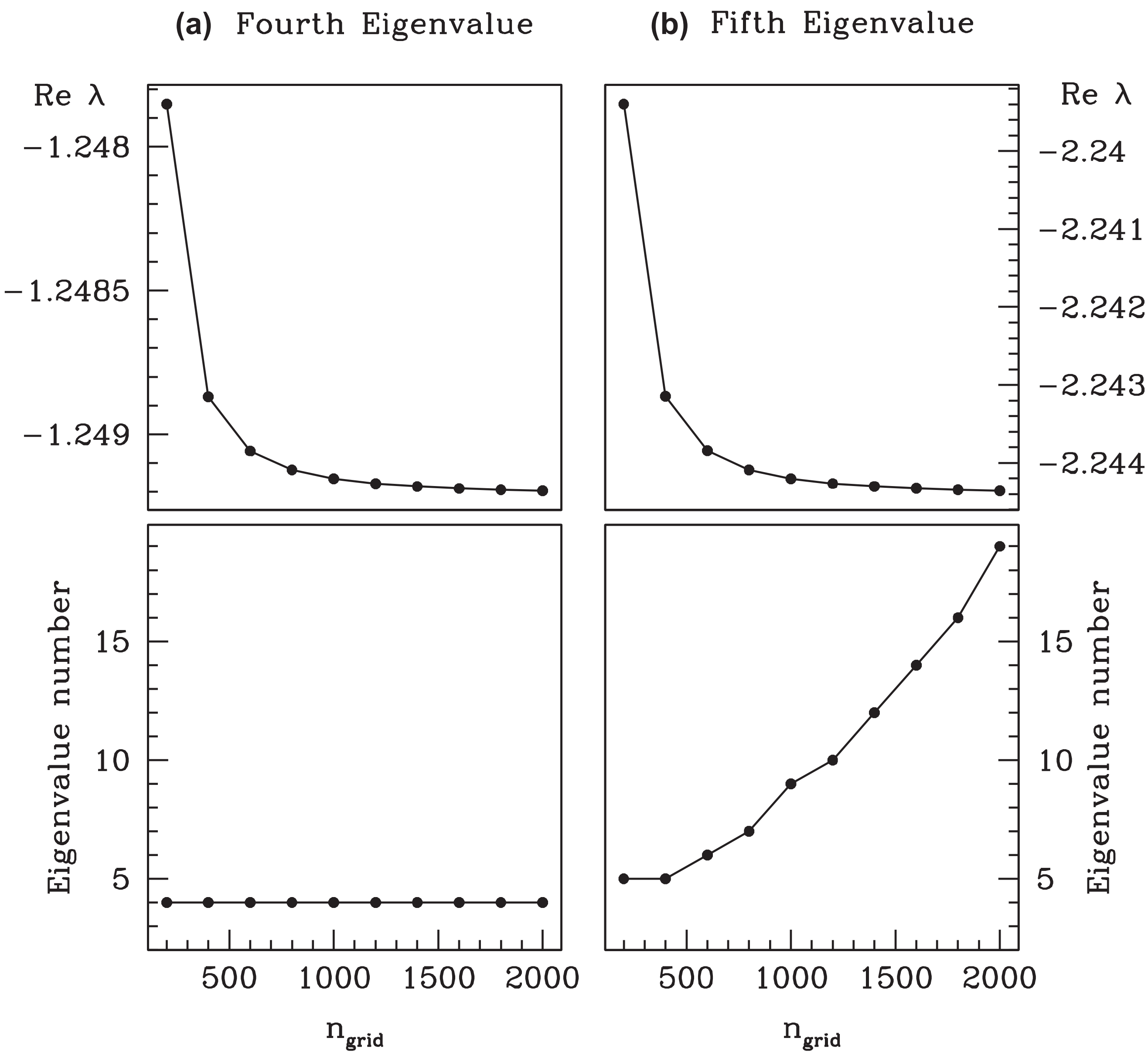

Fig. 6. An illustration of the convergence of matrix eigenvalues to the fourth and fifth eigenvalues (ordered by real part with $\mathrm{Im}\,\lambda \geqslant 0$) of the (unique) PTW solution of (1), for $A = 2.0$, $B = 0.45$, $v = 182.5$ and $c = 0.65$. The upper panels show the real part of the matrix eigenvalue as a function of n_{grid}, which is the number of grid points in the (non-uniform) mesh used to calculate the PTW solution. Since there are two PDE variables, the matrix arising from the discretisation has size $2n_{grid} \times 2n_{grid}$. The lower panels show the number of the matrix eigenvalue that is being plotted in the upper panel, with these eigenvalues being ordered by real part considering only eigenvalues whose imaginary part is positive or approximately zero. In (a), the matrix eigenvalue is number 4 throughout. However in (b), an increasing number of matrix eigenvalues with real part between −1.249209 and −2.244407 and with very large imaginary parts ($\sim 10^4$) arise as the discretisation becomes finer. Consequently the number of the matrix eigenvalue that is plotted in the upper panel gradually increases with n_{grid}. The data for this figure was generated using the WAVETRAIN [37] commands `eigenvalue_convergence` and `convergence_table`; full details are given at [38].

Two new issues arise when there is such a fold. Firstly, one must keep careful track of which of the multiple PTWs is being studied at any given pair of control parameter and wave speed values. The WAVETRAIN package achieves this via an input parameter through which the user specifies whether they wish to study the first/second/third/$\cdots$ wave along the solution branch. Secondly, the region in which PTWs exist may now be bounded in part by the locus of the fold, rather than by the locus of a Hopf bifurcation point or a homoclinic solution. This is the case for (1) in the range $c \approx 21$, as illustrated in Fig. 5. Further details of PTW solutions of (1) for values of c in this range are given in [29].

5.3. Complications in the convergence of matrix eigenvalues

The first stage in the determination of PTW stability is the solution of the matrix eigenvalue problem given by discretising the eigenfunction equation with $\gamma = 0$. Intuitively, one would expect this to give successively better approximations to the PDE eigenvalues and eigenvectors as the discretisation becomes finer, and in many cases there are analytical convergence results that ensure this [54–57]. However more complicated behaviour can occur for some equations, and the Klausmeier model (1) provides an example of this, which I illustrate via one particular case. For parameter values $A = 2.0$, $B = 0.45$, $\nu = 182.5$ and $c = 0.65$, high-accuracy numerical calculations indicate that for (5) and (6), the fourth and fifth eigenvalues (ordered by real part with $\mathrm{Im}\lambda \geqslant 0$) are $-1.249209 + i0.6226896$ and $-2.244407 + i0.8923310$, to seven significant figures. Fig. 6 plots the real and imaginary parts of selected eigenvalues of the matrix given by discretising the eigenfunction equation, using standard three point approximations for the first and second spatial derivatives. As expected, there is convergence in both cases as the number of points in the discretisation increases. In Fig. 6a, the matrix eigenvalue that is plotted is the fourth eigenvalue for all discretisations, ordered by real part considering only eigenvalues whose imaginary part is positive or approximately zero. This is as expected intuitively. However, in Fig. 6b, the eigenvalue that is plotted is only the fifth eigenvalue for relatively coarse discretisations (see lower panel). As the discretisation becomes finer, new eigenvalues appear with real parts between -1.249209 and -2.244407, and with very large imaginary parts ($\sim 10^4$). These appear to be an artifact of the discretisation. In a case such as this, the remedy is simply to exclude matrix eigenvalues with very large imaginary parts from those used as starting points for numerical continuation of the essential spectrum. This facility is available in WAVETRAIN.

5.4. Stability changes of Hopf type

In Section 3.2 I described the use of numerical continuation to calculate the locus of changes in PTW stability of Eckhaus (sideband) type, meaning that the spectrum changes its direction of curvature at the origin. PTWs can also change stability through a transition of Hopf type [53], in which a fold in the spectrum crosses the imaginary axis away from the origin. An example of this is given in [50], in a study of the Oregonator model. Loci of stability changes of Hopf type can also be traced by numerical continuation; this involves a new numerical algorithm that I will present in a separate paper [58]. This new algorithm is implemented by the WAVETRAIN command `stability_boundary`.

6. Discussion

Numerical continuation is a powerful method for studying PTW solutions of PDEs. Moreover the software package WAVETRAIN makes this approach accessible to those without previous experience of numerical continuation.

One important property of PTWs has not yet been mentioned in this paper: absolute stability. A PTW is unstable if suitable small perturbations grow when applied to the wave. These perturbations may move in space as they grow. If all growing perturbations simultaneously move, then the PTW is known as "convectively unstable" – this is a subset of unstable waves. The term "absolutely unstable" is used for PTWs for which there are perturbations that grow without moving. These different types of stability have a major effect on the way in which a PTW can feature in PDE solutions. For example, appropriate initial and boundary conditions can generate solutions containing a permanent moving band of convectively unstable PTWs [7,59–64].

There are two established numerical methods for determining the absolute stability of a PDE solution. The oldest involves tracking saddle points of the dispersion relation in a moving frame of reference [65,66]. Though effective and general, this method is difficult to use in practice. A more recent and simpler alternative method is to calculate the "absolute spectrum" [67,68], which can be done by numerical continuation [18,60]. However the numerical algorithm only applies to spatially uniform solutions. An extension to PTWs is an important objective for future work: the difficulty is not the numerical continuation itself, but the systematic generation of suitable starting points. Note however that there is one important special case is which the absolute stability of PTWs can be determined by numerical continuation: the complex Ginzburg–Landau equation. Here a change of variables can be applied that reduces PTWs to spatially uniform solutions [2]. The resulting absolute stability information has proved extremely valuable in explaining spatiotemporal dynamics in this equation [60,69,70].

Acknowledgements

This work was supported in part by a Leverhulme Trust Research Fellowship.

I thank Lyonell Boulton (Heriot-Watt University) for helpful discussions.

References

[1] N. Kopell, L.N. Howard, Plane wave solutions to reaction–diffusion equations, Stud. Appl. Math. 52 (1973) 291–328.
[2] I.S. Aranson, L. Kramer, The world of the complex Ginzburg–Landau equation, Rev. Mod. Phys. 74 (2002) 99–143.
[3] R.E.L. DeVille, E. Vanden-Eijnden, Wavetrain response of an excitable medium to local stochastic forcing, Nonlinearity 20 (2007) 51–74.
[4] J.A. Sherratt, G.J. Lord, Nonlinear dynamics and pattern bifurcations in a model for vegetation stripes in semi-arid environments, Theor. Popul. Biol. 71 (2007) 1–11.
[5] V. Steinberg, J. Fineberg, E. Moses, I. Rehberg, Pattern selection and transition to turbulence in propagating waves, Physica D 37 (1989) 359–383.
[6] M. van Hecke, Coherent and incoherent structures in systems described by the 1D CGLE: experiments and identification, Physica D 174 (2003) 134–151.
[7] W. van Saarloos, Front propagation into unstable states, Phys. Rep. 386 (2003) 29–222.
[8] M.R.E. Proctor, S.M. Tobias, E. Knobloch, Noise-sustained structures due to convective instability in finite domains, Physica D 145 (2000) 191–206.
[9] N. Kopell, L.N. Howard, Horizontal bands in Belousov reaction, Science 180 (1973) 1171–1173.
[10] I.R. Epstein, K. Showalter, Nonlinear chemical dynamics: oscillations, patterns and chaos, J. Phys. Chem. 100 (1996) 13132–13147.
[11] V.K. Vanag, I.R. Epstein, Design and control of patterns in reaction–diffusion systems, Chaos 18 (2008) (Art. No. 026107).
[12] G. Bordyugov, N. Fischer, H. Engel, N. Manz, O. Steinbock, Anomalous dispersion in the Belousov–Zhabotinsky reaction: experiments and modeling, Physica D 239 (2010) 766–775.
[13] E. Ranta, V. Kaitala, Travelling waves in vole population dynamics, Nature 390 (1997) 456.
[14] S.M. Bierman, J.P. Fairbairn, S.J. Petty, D.A. Elston, D. Tidhar, X. Lambin, Changes over time in the spatiotemporal dynamics of cyclic populations of field voles (*Microtus agrestis* L.), Am. Nat. 167 (2006) 583–590.
[15] J.A. Sherratt, M.J. Smith, Periodic travelling waves in cyclic populations: field studies and reaction–diffusion models, J. R. Soc. Interf. 5 (2008) 483–505.
[16] C. Valentin, J.M. d'Herbès, J. Poesen, Soil and water components of banded vegetation patterns, Catena 37 (1999) 1–24.
[17] M. Rietkerk, S.C. Dekker, P.C. de Ruiter, J. van de Koppel, Self-organized patchiness and catastrophic shifts in ecosystems, Science 305 (2004) 1926–1929.
[18] J.D.M. Rademacher, B. Sandstede, A. Scheel, Computing absolute and essential spectra using continuation, Physica D 229 (2007) 166–183.
[19] C.A. Klausmeier, Regular and irregular patterns in semiarid vegetation, Science 284 (1999) 1826–1828.
[20] <http://indy.cs.concordia.ca/auto>.
[21] E.J. Doedel, Auto, a program for the automatic bifurcation analysis of autonomous systems, Cong. Numer. 30 (1981) 265–384.
[22] E.J. Doedel, H.B. Keller, J.P. Kernévez, Numerical analysis and control of bifurcation problems: (I) Bifurcation in finite dimensions, Int. J. Bifurcat. Chaos 1 (1991) 493–520.
[23] E.J. Doedel, W. Govaerts, Y.A. Kuznetsov, A. Dhooge, Numerical continuation of branch points of equilibria and periodic orbits, in: E.J. Doedel, G. Domokos, I.G. Kevrekidis (Eds.), Modelling and Computations in Dynamical Systems, World Scientific, Singapore, 2006, pp. 145–164.
[24] R.M. Callaway, Positive interactions among plants, Bot. Rev. 61 (1995) 306–349.
[25] M. Rietkerk, P. Ketner, J. Burger, B. Hoorens, H. Olff, Multiscale soil and vegetation patchiness along a gradient of herbivore impact in a semi-arid grazing system in West Africa, Plant Ecol. 148 (2000) 207–224.
[26] N. Ursino, The influence of soil properties on the formation of unstable vegetation patterns on hillsides of semiarid catchments, Adv. Water Resour. 28 (2005) 956–963.
[27] J.A. Sherratt, An analysis of vegetation stripe formation in semi-arid landscapes, J. Math. Biol. 51 (2005) 183–197.
[28] J.A. Sherratt, Pattern solutions of the Klausmeier model for banded vegetation in semi-arid environments I, Nonlinearity 23 (2010) 2657–2675.
[29] J.A. Sherratt, Pattern solutions of the Klausmeier model for banded vegetation in semi-arid environments II: Patterns with the largest possible propagation speeds, Proc. R. Soc. Lond. A 467 (2011) 3272–3294.
[30] J.A. Sherratt, Pattern solutions of the Klausmeier model for banded vegetation in semi-arid environments III: the transition between homoclinic solutions, submitted for publication.
[31] R. Lefever, O. Lejeune, On the origin of tiger bush, Bull. Math. Biol. 59 (1997) 263–294.
[32] R. HilleRisLambers, M. Rietkerk, F. van de Bosch, H.H.T. Prins, H. de Kroon, Vegetation pattern formation in semi-arid grazing systems, Ecology 82 (2001) 50–61.
[33] J. von Hardenberg, E. Meron, M. Shachak, Y. Zarmi, Diversity of vegetation patterns and desertification, Phys. Rev. Lett. 87 (2001) (Art. No. 198101).
[34] M. Rietkerk, M.C. Boerlijst, F. van Langevelde, R. HilleRisLambers, J. van de Koppel, H.H.T. Prins, A. de Roos, Self-organisation of vegetation in arid ecosystems, Am. Nat. 160 (2002) 524–530.
[35] E. Gilad, J. von Hardenberg, A. Provenzale, M. Shachak, E. Meron, A mathematical model of plants as ecosystem engineers, J. Theor. Biol. 244 (2007) 680–691.
[36] F. Borgogno, P. D'Odorico, F. Laio, L. Ridolfi, Mathematical models of vegetation pattern formation in ecohydrology, Rev. Geophys. 47 (2009) (Art. No. RG1005).
[37] <http://www.ma.hw.ac.uk/wavetrain>.
[38] <http://www.ma.hw.ac.uk/~jas/supplements/numericalcontinuation>.
[39] M.J. Smith, J.A. Sherratt, The effects of unequal diffusion coefficients on periodic travelling waves in oscillatory reaction–diffusion systems, Physica D 236 (2007) 90–103.
[40] R.H. Wang, Q.X. Liu, G.Q. Sun, Z. Jin, J. van de Koppel, Nonlinear dynamic and pattern bifurcations in a model for spatial patterns in young mussel beds, J. R. Soc. Interf. 6 (2009) 705–718.
[41] A.R. Champneys, Y.A. Kuznetsov, Numerical detection and continuation of codimension-two homoclinic bifurcations, Int. J. Bifurcat. Chaos 4 (1994) 785–822.
[42] A.R. Champneys, Y.A. Kuznetsov, B. Sandstede, A numerical toolbox for homoclinic bifurcation analysis, Int. J. Bifurcat. Chaos 6 (1996) 867–887.
[43] B. Deconinck, J.N. Kutz, Computing spectra of linear operators using the Floquet–Fourier–Hill method, J. Comput. Phys. 219 (2006) 296–321.
[44] R.A. Gardner, On the structure of the spectra of periodic travelling waves, J. Math. Pure Appl. 72 (1993) 415–439.
[45] B. Sandstede, Stability of travelling waves, in: B. Fiedler (Ed.), Handbook of Dynamical Systems II, North-Holland, Amsterdam, 2002, pp. 983–1055.
[46] <http://www.caam.rice.edu/software/ARPACK>.
[47] R.B. Lehoucq, D.C. Sorensen, C. Yang, Arpack Users' Guide: Solution of Large-Scale Eigenvalue Problems with Implicitly Restarted Arnoldi Methods, Society for Industrial and Applied Mathematics, Philadelphia, 1998.
[48] <http://www.netlib.org/lapack>.
[49] E. Anderson, Z. Bai, C. Bischof, S. Blackford, J. Demmel, J. Dongarra, J. Du Croz, A. Greenbaum, S. Hammarling, A. McKenney, D. Sorensen, Lapack Users' Guide, third ed., Society for Industrial and Applied Mathematics, Philadelphia, 1999.
[50] G. Bordiougov, H. Engel, From trigger to phase waves and back again, Physica D 215 (2006) 25–37.
[51] B. Deconinck, F. Kiyak, J.D. Carter, J.N. Kutz, SpectrUW: a laboratory for the numerical exploration of spectra of linear operators, Math. Comput. Simulat. 74 (2007) 370–379.
[52] <http://www.amath.washington.edu/hill/spectruw.html>.
[53] J.D.M. Rademacher, A. Scheel, Instabilities of wave trains and Turing patterns in large domains, Int. J. Bifurcat. Chaos 17 (2007) 2679–2691.
[54] F.V. Atkinson, Discrete and Continuous Boundary Problems, Academic Press, New York, 1964.
[55] H.O. Kreiss, Difference approximation for boundary and eigenvalue problems for ordinary differential equations, Math. Comput. 26 (1972) 605–624.

[56] C. de Boor, B. Swartz, Collocation approximation to eigenvalues of an ordinary differential equation: the principle of the thing, Math. Comput. 35 (1980) 679–694.
[57] F. Chatelin, The spectral approximation of linear operators with applications to the computation of eigenelements of differential and integral operators, SIAM Rev. 23 (1981) 495–522.
[58] J.A. Sherratt, Numerical continuation of boundaries in parameter space between stable and unstable periodic travelling wave (wavetrain) solutions of partial differential equations, submitted for publication.
[59] J.A. Sherratt, Unstable wavetrains and chaotic wakes in reaction–diffusion systems of λ–ω type, Physica D 82 (1995) 165–179.
[60] M.J. Smith, J.D.M. Rademacher, J.A. Sherratt, Absolute stability of wavetrains can explain spatiotemporal dynamics in reaction–diffusion systems of lambda-omega type, SIAM J. Appl. Dyn. Syst. 8 (2009) 1136–1159.
[61] K. Nozaki, N. Bekki, Pattern selection and spatiotemporal transition to chaos in the Ginzburg–Landau equation, Phys. Rev. Lett. 51 (1983) 2171–2174.
[62] S.V. Petrovskii, H. Malchow, Wave of chaos: new mechanism of pattern formation in spatio-temporal population dynamics, Theor. Popul. Biol. 59 (2001) 157–174.
[63] M.R. Garvie, Finite difference schemes for reaction–diffusion equations modeling predator–prey interactions in MATLAB, Bull. Math. Biol. 69 (2007) 931–956.
[64] S.M. Merchant, W. Nagata, Wave train selection behind invasion fronts in reaction–diffusion predator–prey models, Physica D 239 (2010) 1670–1680.
[65] L. Brevdo, Convectively unstable wave packets in the Blasius boundary layer, Z. Angew. Math. Mech. 75 (1995) 423–436.
[66] L. Brevdo, P. Laure, F. Dias, T.J. Bridges, Linear pulse structure and signalling in a film flow on an inclined plane, J. Fluid Mech. 396 (1999) 37–71.
[67] B. Sandstede, A. Scheel, Absolute versus convective instability of spiral waves, Phys. Rev. E 62 (2000) 7708–7714.
[68] B. Sandstede, A. Scheel, Absolute and convective instabilities of waves on unbounded and large bounded domains, Physica D 145 (2000) 233–277.
[69] J.A. Sherratt, M.J. Smith, J.D.M. Rademacher, Locating the transition from periodic oscillations to spatiotemporal chaos in the wake of invasion, Proc. Natl. Acad. Sci. USA 106 (2009) 10890–10895.
[70] M.J. Smith, J.A. Sherratt, Propagating fronts in the complex Ginzburg–Landau equation generate fixed-width bands of plane waves, Phys. Rev. E 80 (2009) (Art. No. 046209).